Studies on F^{19} in the $O^{18}(p,\gamma)F^{19}$ Reaction*†

J. P. ALLEN, A. J. HOWARD‡, AND D. A. BROMLEY
Nuclear Structure Laboratory, Yale University, New Haven, Connecticut

AND

J. W. OLNESS
Brookhaven National Laboratory, Upton, New York

(Received 22 July 1965)

Studies of the $O^{18}(p,\gamma)F^{19}$ reaction at the 849-keV resonance have established decay schemes for the 8.76-MeV resonance level and also for the 3.91-MeV level which is populated through de-excitation of the former by an 18% branch. Angular-correlation measurements establish a $J=\frac{3}{2}$ assignment for the 3.91-MeV level. A level of this spin assignment is not predicted by the intermediate-coupling shell models, but all collective models which have been applied to F^{19} and which imply a strong prolate deformation of the nucleus have predicted a $\frac{3}{2}^+$ state in this energy region. Selection rules based on the asymptotic Nilsson model provide an excellent description of the de-excitation branching ratios for both the 8.76- and the 3.91-MeV state as studied herein, demonstrating the utility of these rules even in so light a nucleus. Additional measurements at the 1169-keV resonance have determined the decay scheme for the 9.07-MeV resonance level, which deexcites strongly through the 2.79-MeV level. The limitation $J=\frac{5}{2}$ or $\frac{9}{2}$ on possible spin assignments for the 2.79-MeV level is confirmed; however, simple angular-distribution measurements cannot distinguish between these two possibilities.

I. INTRODUCTION

EXTENSIVE interest in the static and dynamic properties of the low levels of F^{19} has followed the pioneering calculations of Paul[1] demonstrating the remarkable similarity between a strong-coupling collective-model[2] interpretation of the available data and the predictions obtained by Elliott and Flowers[3] and by Redlich[4] on the basis of a spherical-shell model including configuration mixing. This similarity led to the work by Elliott[5] on the SU_3 classification of shell-model states to yield collective characteristics, and to a greatly increased understanding of the general relationships between collective and independent particle motions in the nucleus. A wide variety of more recent calculations, emphasizing one or another of these aspects of behavior, has been reported for the F^{19} level spectrum. Among these are the calculations of Chi and Davidson,[6] of Inoue *et al.*,[7] and of Harvey.[8]

Many of the characteristics of the low states of F^{19} have been known for some time; however, recent detailed $(p,p'\gamma)$ and other studies by Prentice *et al.*[9] have established unambiguous assignments to the first six states up to and including the $\frac{3}{2}^+$, 1.56-MeV state. These measurements have provided the basis for a remarkably successful collective-model interpretation of these states as representing highly decoupled, overlapping, positive- and negative-parity $K=\frac{1}{2}$ rotational bands. Although the next higher lying state at 2.79-MeV has long been associated with the low-lying $J^\pi=\frac{9}{2}^+$ level predicted by both the shell-model[3,4] and the collective-model[1] calculations, a rigorous determination of its spin and parity has not yet been reported. Huang *et al.*[10] have set forth a $J=\frac{9}{2}$ assignment from gamma-ray angular-distribution measurements in the $O^{18}(p,\gamma)F^{19}$ reaction. However, the present experiment casts some doubt on their conclusions, and hence this suggested assignment must be reconsidered. However, their results[10] do provide a rigorous restriction on possible spin values of $J\geqslant\frac{5}{2}$. Although the work of Freeman[11] on the $F^{19}(n,n'\gamma)F^{19}$ reaction cannot rigorously exclude a $J=\frac{5}{2}$ assignment, a preference is suggested for possible assignments of $J=\frac{7}{2}$ or $J=\frac{9}{2}$.

At excitation energies in excess of 5 MeV, extensive experimental data on F^{19} states have been obtained in studies on the $N^{15}+\alpha$ and $O^{18}+p$ reactions[12–14]; in the intervening region between 3 and 5 MeV, however, essentially no data beyond the excitation energies have as yet been reported for some six states. These states are of particular interest in any attempt to elucidate the relative validity of the model variants which have been

* Work supported in part by the U. S. Atomic Energy Commission.

† The research reported herein was submitted by J. P. Allen in partial fulfillment of the requirement for the Ph.D. degree at Yale University, 1965.

‡ Summer Research Associate. Permanent address: Trinity College, Hartford, Connecticut.

[1] E. B. Paul, Phil. Mag. **15**, 311 (1957).
[2] S. G. Nilsson, Kgl. Danske Videnskab. Selskab, Mat. Fys. Medd. **29**, No. 16 (1955).
[3] J. P. Elliott and B. H. Flowers, Proc. Roy. Soc. (London) **A229**, 536 (1955).
[4] M. G. Redlich, Phys. Rev. **99**, 1427 (1955).
[5] J. P. Elliott, Proc. Roy. Soc. (London) **A245**, 128 (1958).
[6] B. E. Chi and J. P. Davidson, Phys. Rev. **131**, 366 (1963).
[7] T. Inoue, T. Sebe, H. Hagiwara, and A. Arima (to be published).
[8] M. Harvey, Nucl. Phys. **52**, 542 (1964).
[9] J. D. Prentice, N. W. Gebbie, and H. S. Caplan, Phys. Letters **3**, 201 (1963).
[10] K. Huang, K. Yagi, T. Awaya, H. Ohnuma, M. Fujioka, and Y. Nogami, J. Phys. Soc. Japan **18**, 646 (1963).
[11] J. M. Freeman, Phil. Mag. **2**, 628 (1957).
[12] H. Smotrich, K. W. Jones, L. C. McDermott, and R. E. Benenson, Phys. Rev. **122**, 232 (1961).
[13] R. R. Carlson, C. C. Kim, J. A. Jacobs, and A. C. L. Bernard, Phys. Rev. **122**, 607 (1961).
[14] K. Yagi, K. Katori, H. Ohnuma, Y. Hashimoto, and Y. Nogami, J. Phys. Soc. Japan **17**, 595 (1964).

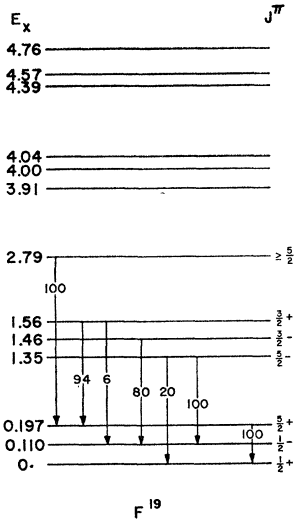

FIG. 1. Partial energy-level diagram of F^{19} showing the experimental de-excitation scheme of the lower levels. Energies are expressed in MeV. Contrary to what is shown in the figure, the 20% branch should originate from the 1.46-MeV state.

evolved for this mass region. Although all such models effectively give overlapping predictions for the states below 3 MeV and are not distinguishable in that range, the predictions diverge in striking fashion for higher excitations as will be discussed below. The available experimental evidence on these levels is summarized in Fig. 1.

The measurements to be reported herein were carried out in an attempt to provide spectroscopic information on these states. In particular, in this paper, we report on a detailed study of the 849-keV resonance in the $O^{18}(p,\gamma)F^{19}$ reaction. Previous studies on the elastic scattering of protons in this energy range by Carlson *et al.*[13] and by Yagi *et al.*[14] have demonstrated that this resonance has a $\frac{1}{2}^+$ assignment making it particularly attractive in terms of correlation studies on cascade de-excitations. Measurements on the radiative capture reaction have been reported previously by Huang *et al.*,[10] by Butler and Holmgren,[15] and by Nelson and Hudspeth.[16] However, in these measurements attention has been directed to those resonances which deexcited almost exclusively via the low-lying triplet states in F^{19}; and no detailed studies have been reported on resonances, including that at 849 keV, which demonstrated a more complex deexcitation. Incidental to the information which has been obtained concerning the angular momentum and deexcitation branching of the 3.91-MeV state has been a determination of the branching from the resonance itself.

A similar study of the 1169-keV resonance was carried out to determine the decay scheme of the 9.07-MeV resonance level which has not been previously established. Gamma-ray angular distribution measurements were also undertaken in order to investigate possible conclusions with respect to the spin and parity of the 2.79-MeV level, which is populated strongly in the de-excitation of the resonance level.

It has been shown previously by Yagi[17] through analysis of the $O^{18}(p,p)O^{18}$ cross section that the 9.07-MeV level is formed by g-wave ($l=4$) protons and hence has definite even parity and spin $J=\frac{7}{2}$ or $J=\frac{9}{2}$. Amsel and Bishop[18] have observed the α_0 group from the $O^{18}(p,\alpha)N^{15}$ reaction. On the basis of a significant $P_6(\cos\theta)$ dependence in the measured α_0 angular distribution they conclude that the level has $J=\frac{7}{2}$. Although a preference is expressed for an odd-parity assignment, their results are not inconsistent with the even-parity assignment required by Yagi's analysis.[17] The reasons for excluding a possible $J=\frac{9}{2}$ assignment from consideration are not discussed in their paper, however.

II. INVESTIGATION OF THE 849-keV RESONANCE LEVEL

A. General Procedure

A gas target cell containing 99.5% isotopically pure O^{18} gas at 20 cm of mercury pressure was bombarded with protons from the Brookhaven 4-MeV Van de Graaff accelerator. The proton beam entered the target volume through a 0.00025-cm nickel-foil window and the beam energy was regulated by passing the HH^+ beam, simultaneously accelerated, through a 60° electrostatic analyzer to the accelerator servo-control slits. In order to minimize carbon build-up on the entrance window of the target cell, a liquid-nitrogen-filled annular trap was installed in the beam line immediately forward of the target.

Gamma radiation was detected using two standard 5-in.-diam×5-in. NaI(Tl) spectrometers having a measured energy resolution of 9.2% for the 661-keV Cs^{137} line. Standard transistorized instrumentation was used throughout, including stabilizers operating on

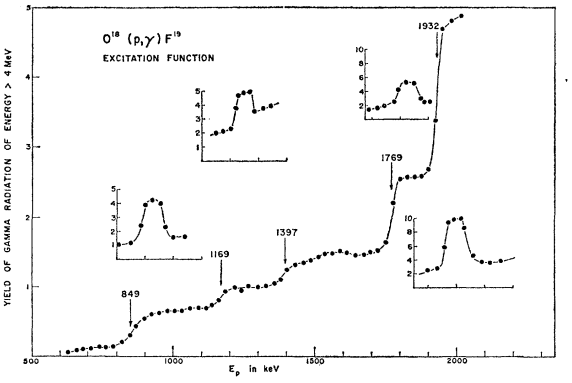

FIG. 2. Excitation function for $O^{18}(p,\gamma)F^{19}$ with yield of gamma radiation of energy greater than 4 MeV plotted against proton energy in kiloelectron volts. The gas target pressure was 20 cm of Hg absolute for the main curve; 3.8 cm of Hg for the inset curves.

[15] J. W. Butler and H. D. Holgmgren, Phys. Rev. **116**, 1485 (1959).
[16] J. W. Nelson and E. L. Hudspeth, Phys. Rev. **125**, 301 (1962).
[17] K. Yagi, J. Phys. Soc. Japan **17**, 604 (1964).
[18] G. Amsel and G. R. Bishop, Phys. Rev. **123**, 957 (1961).

prominent spectrum lines to control the applied voltage to, hence the gain of, the photomultiplier assemblies. In coincidence measurements to establish de-excitation characteristics and branching ratios, the crystals were mounted at $\pm 90°$ to the proton beam with their front faces 2.5 cm from the reaction volume, thus effectively averaging anisotropies in the angular distributions. In angular-correlation measurements a face-to-reaction volume distance of 12 cm was used and the correlation coefficients were appropriately corrected[19] for the finite solid angles involved.

A typical excitation function for all gamma radiation of energy greater than 4 MeV is shown in Fig. 2. The indicated proton energy scale has been corrected for loss in the window and target gas to give the resultant energy at the center of the target volume. The resonances in this excitation function at 849, 1169, 1397, 1769, and 1932 keV have also been reported by Butler and Holmgren[15] and by Nelson and Hudspeth,[16] among others. The resonance widths shown in the insets in this figure are purely instrumental, reflecting the finite target thickness. In the present measurements the electrostatic analyzer scale was calibrated by observation of the 4.43-MeV gamma radiation from the $N^{15}(p,\alpha\gamma)C^{12}$ reaction induced by an air filling of the target volume. In particular, the known resonances[20] at 429 ± 1, 898 ± 1 and 1210 ± 3 keV have been used to establish this calibration.

B. Branching Ratio Determinations

The 849-keV resonance has been examined in detail using a beam current of approximately 1 μA, limited by the transmission capabilities of the nickel-target window for long bombardments. Figure 3 presents a direct gamma-radiation spectrum obtained in one of the 5-in. diam$\times$5-in. NaI(Tl) spectrometers under the conditions

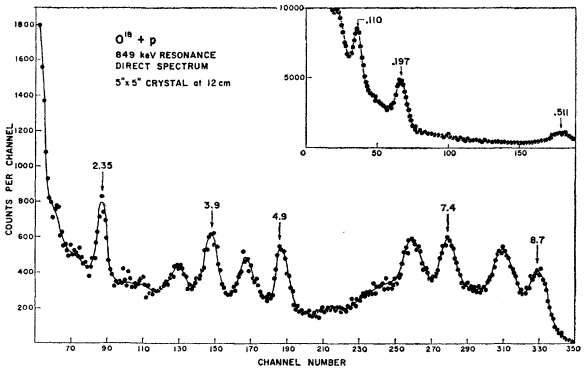

FIG. 3. $O^{18}+p$ direct gamma-radiation spectrum at $E_p=849$ keV. Approximate energies are indicated in MeV. The inset shows a high-grain (low-energy) spectrum at the same resonance.

[19] J. B. Marion, *Nuclear Data Tables* (National Academy of Sciences—National Research Council, Washington, D. C., 1960), Part 3.

[20] F. Ajzenberg-Selove and T. Lauritsen, Nucl. Phys. 11, 1 (1955).

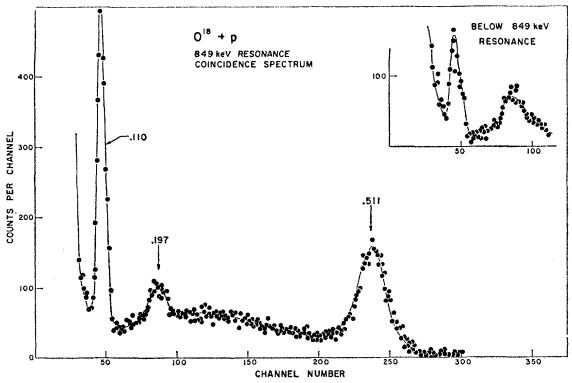

FIG. 4. $O^{18}+p$ gamma radiation spectrum at $E_p=849$ keV in time coincidence with the 8.7-MeV transition into the ground-state triplet. Energies are in MeV. The inset displays a portion of a spectrum obtained under similar conditions except with the proton energy 100 keV below the resonance energy ($E_p\cong750$ keV).

specified above. The energy scale calibration was accomplished using standard radioactive sources (Co^{60}, ThC'', and Pu-Be) in addition to radiations of known energy from the 1769- and 1932-keV capture resonances for $O^{18}+p$.

The system resolution is clearly inadequate to resolve the primary transitions to members of the low-lying triplets. However, the spectrum of Fig. 3 indicates strong transitions of mean energies 8.7 and 7.4 MeV, corresponding to primary de-excitation transitions to one or more members of each of the triplets.

In order to establish the substructure of these transitions, coincidence measurements were carried out using the two 5-in.$\times$5-in. NaI spectrometers. To minimize spurious coincidences a 0.5-in. lead filter was inserted between the target and the crystal on whose output voltage gates, defining the high-energy member of the coincidence cascades, were established.

During each coincidence measurement the real-to-random coincidence corrections were examined by insertion of a fixed 0.4-μsec delay in one channel of the fast coincidence circuit. Operating with a resolving time of some 50 nsec it was found that the accidental coincidence rate was entirely negligible. Off-resonance measurements at energies just below the 849-keV resonance established that corrections reflecting real coincidences from nonresonant capture situations were also negligible except where specifically included hereafter. Through use of a parallel multichannel analyzers and voltage gates, it was possible to record several coincidence spectra simultaneously.

The direct gamma radiation spectrum in Fig. 3 shows strong radiations of energies $\sim$8.7, $\sim$7.4, 4.9, 3.91, and 2.35 MeV corresponding to de-excitation of the capture state to members of the low triplets and to a state at 3.91 MeV. Evidence that a state at 4.85 MeV was not involved is obtained directly from the fact that the intensity of the 3.91-MeV radiation is significantly less than that of the 4.85-MeV radiation, reflecting branch-

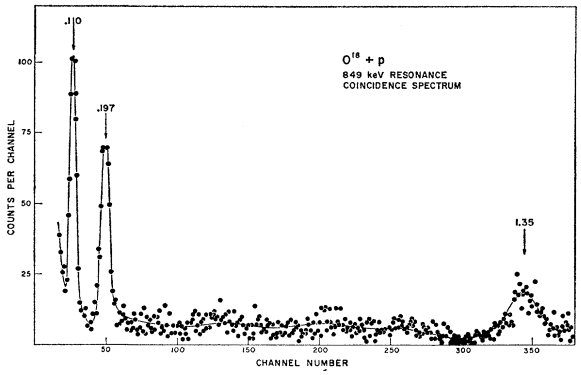

FIG. 5. $O^{18}+p$ gamma radiation spectrum at $E_p=849$ keV in time coincidence with the 7.4-MeV transition into the first excited triplet.

ing in the de-excitation of the 3.91-MeV state. This figure also includes an expanded spectrum of the low-energy direct radiation showing radiations of 0.110 and 0.197 MeV, which are involved in the cascade de-excitations, together with the omnipresent annihilation radiation.

In order to separate transitions to individual members of the low-lying triplets and to elucidate the de-excitation further, a systematic program of gamma-gamma coincidence studies was undertaken as described previously.

Figure 4 is a spectrum measured in coincidence with a voltage gate set on the photopeak of the ~8.7-MeV radiation. The dominant 0.110-MeV transition observed demonstrates that the de-excitation proceeds strongly via a direct cascade involving the first excited state. From the known efficiency of the spectrometers for gamma radiation in the energy range of interest, these data, and others to be presented in subsequent figures, were analyzed to provide the detailed branching ratios. This figure demonstrates the absence, within experimental accuracy, of any direct $E2$ transitions to the $\frac{5}{2}+$

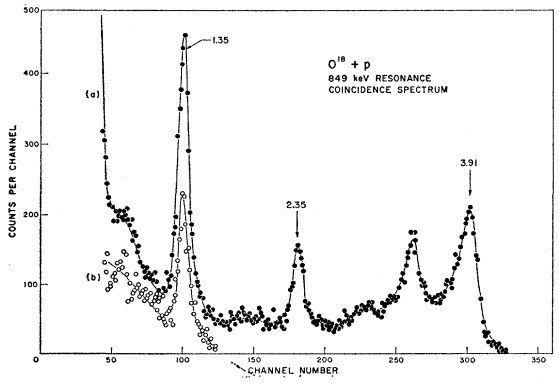

FIG. 6. $O^{18}+p$ gamma-radiation spectrum at $E_p=849$ keV in time coincidence with the 4.85-MeV transition. Careful energy calibration of this spectrum and the direct gamma spectrum establish the prominent 4.9- and 3.9-MeV radiations as members of the two-step cascade through the 3.91-MeV state. The open circles indicate the coincident spectrum obtained with a similar voltage gate set just above the 4.85-MeV photopeak.

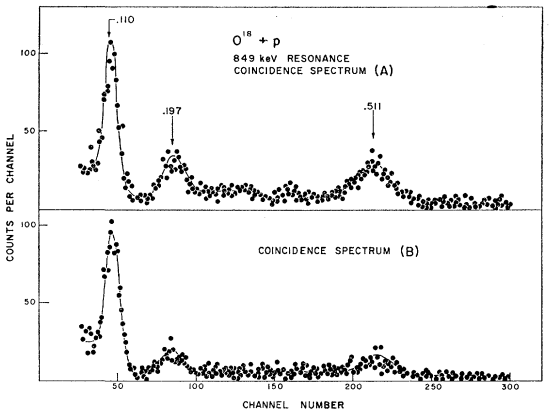

FIG. 7. (A) $O^{18}+p$ gamma-radiation spectrum at high gain obtained under the same conditions as in Fig. 6, and (B) gamma-radiation spectrum obtained under conditions identical to (A) except with the voltage gate set just above the 4.85-MeV photopeak.

state at 197 keV since the observed 197-keV peak intensity has been shown to be entirely attributable to nonresonant capture. Figure 4 also shows the corresponding spectrum measured at a proton energy 100 keV below the resonance.

Figure 5 presents the gamma radiation spectrum coincident with radiation ~7.4 MeV showing 0.110-, 0.197-, and 1.35-MeV transitions. From the relative intensity of the 0.110- and 0.197-MeV radiations, corrected for real, but unwanted, coincidence yield from the tails of higher energy gamma-radiation pulse-height distributions falling within the voltage gate and the known detailed de-excitation characteristics of the triplet states in F^{19}, it has been possible to obtain the branching shown in a later summary diagram. The absence of any significant 0.511-MeV radiation in this spectrum taken with opposed 5-in.-diam×5-in. NaI crystals demonstrated the effectiveness of the intercrystal lead filter in removing these coincidences.

Figure 6 shows the spectrum coincident with 4.85-MeV radiation composing primarily transitions of 3.91, 2.35, and 1.35 MeV from the 3.91-MeV state and, for comparison, the spectrum obtained with an identical voltage gate set just above the 4.85-MeV photopeak. Figure 7 presents expanded low-energy sections of these spectra showing the 0.110- and 0.197-MeV radiation. Comparison of these spectra indicates that the 3.91-MeV state has no large branch to the first or second excited states and that the observed 0.110- and 0.197-MeV radiations are largely in coincidence with higher radiation tails falling in the coincidence gate apart from a cascade contribution from de-excitation via the upper triplet members. It should be mentioned, however, that the intense 8.7-MeV transition into the 0.110-MeV state leads to a large number of unwanted 0.110- and 8.7-MeV tail coincidences which complicates an accurate determination of the relative branches from the 3.91-MeV state into the ground and first excited states. In order to investigate this problem more fully, a two-parameter

analysis was undertaken following the procedures outlined in Sec. III. The results substantiate the conclusion that the 3.91-MeV level decays predominantly to the ground state, and an upper limit of 10% is placed on possible transitions to the 110-keV level.

Figure 8 presents coincident spectra with gates set on, and immediately above, the 0.197-MeV photopeak. Intensity analysis of these spectra corroborates the branching ratios established from the above spectra.

Figure 9 presents similar results obtained by gating on, and immediately above, the 0.110-MeV photopeak. In particular, this spectrum confirms the dominance of the cascade de-excitations involving this 0.110-MeV state.

In the analysis of all the above spectra, standard spectral shapes, determined using appropriate radioactive sources and the 5-in.×5-in. NaI(Tl) spectrometers, have been used together with efficiency data interpolated from those of Vegors *et al.*[21] Figure 10 presents the branching ratios determined from the present measurements for the 8.76- and 3.91-MeV states in F^{19}.

C. Angular-Correlation Measurement

Since the resonance of $\frac{1}{2}^+$ is firmly established from the elastic proton scattering measurements, the cascade correlations are necessarily functions only of the dihedral angle between the counter axes, independent of the beam orientation. Furthermore, observation of direct radiations from this resonance provided a convenient means of centering the correlation table about the reaction volume. The direct gamma radiations were found to be isotropic to within 0.5.% The correlation between the 4.85- and 3.91-MeV radiations was effectively measured twice by establishing gates on both of these transitions in the counter fixed at 90° to the incident beam and recording the coincident spectra from the moving counter in two parallel multichannel analyzers.

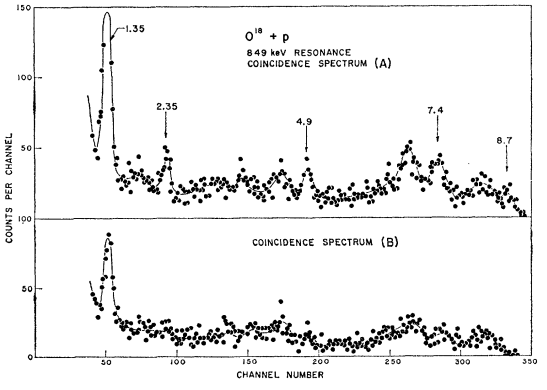

FIG. 8. (A) $O^{18}+p$ gamma-radiation spectrum in time coincidence with the 0.197-MeV transition, and (B) gamma radiation spectrum obtained under conditions identical to (A) except with the voltage gate set just above the 0.197-MeV photopeak.

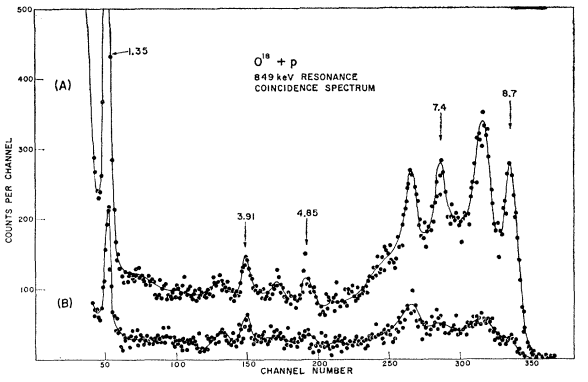

FIG. 9. (A) $O^{18}+p$ gamma radiation spectrum in time coincidence with the 0.110-MeV transition, and (B) gamma-radiation spectrum obtained under conditions identical to (A) except with the voltage gate set just above the 0.110-MeV photopeak. To facilitate comparison, spectrum (B) has been expanded vertically by a factor of 2.

Figure 11 shows the correlation obtained, a theoretical least-squares fit of the function

$$W(\theta)=1+A_2/A_0P_2(\cos\theta)+A_4/A_0P_4(\cos\theta)$$

to the correlation data, and a schematic illustration of

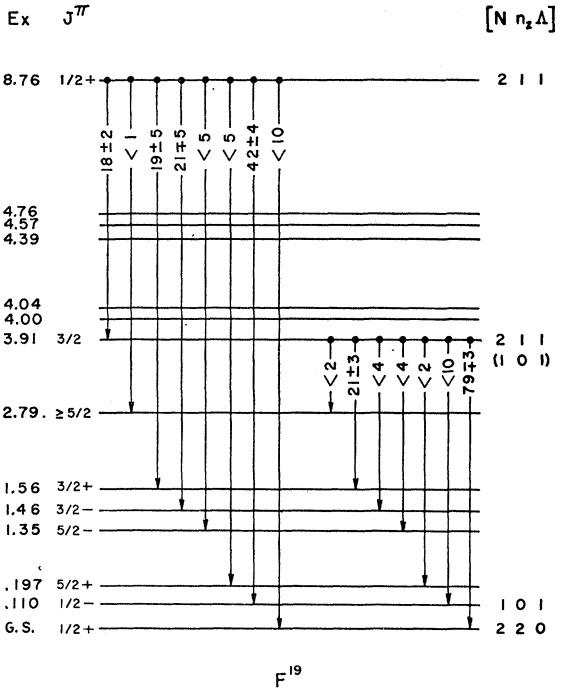

FIG. 10. Energy-level spectrum of F^{19} including the de-excitation branching ratios of the states of 8.76 and 3.91 MeV. Relative transition intensities are indicated in percent with 100% comprising the total gamma de-excitation of a state. Excitation energies in mega-electron-volts and J^π assignments are shown on the left. The asymptotic Nilsson-model quantum numbers $|Nn_z\Lambda\rangle$, which have been identified in the text with particular F^{19} states, are included for easy reference.

[21] S. H. Vegors, L. L. Marsden, and R. L. Heath, Phillips Petroleum Company Report No. IDO-16370, 1958 (unpublished).

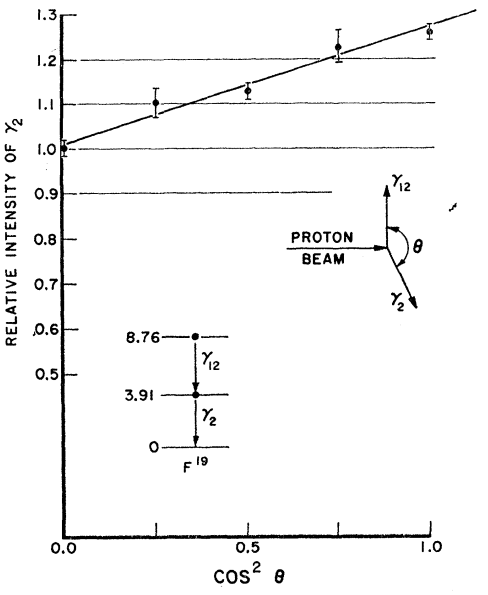

FIG. 11. Angular correlation of the $8.76 \rightarrow 3.91 \rightarrow 0$ MeV cascade de-excitations in the $O^{18}(p,\gamma_{12}\gamma_2)F^{19}$ reaction with $E_p=849$ keV. The solid curve is the result of the least-squares fit to the data of the correlation function given in the text.

the geometry used in the measurement. The coefficient ratio A_4/A_0 is zero within the accuracy of this measurement whereas $A_2/A_0=0.22\pm0.03$ after correction[19] for finite solid angle of the spectrometers.

Correlation measurements on other cascades from this resonance were not examined in detail since all the levels involved have previously received unambiguous assignments.

D. Angular Momentum of the 3.91-MeV State

The intensity of the primary transition to the 3.91-MeV state (18% as shown in Fig. 10) and the anisotropy of the measured $8.76 \rightarrow 3.91 \rightarrow 0$ correlation (as shown in Fig. 11) limit the possible angular-momentum assignments of the 3.91-MeV state to $\frac{3}{2}$ or $\frac{5}{2}$. $J \geqslant \frac{7}{2}$ is excluded specifically from the radiation strength of the 4.85-MeV gamma ray, which requires that it be predominantly $L \leqslant 2$.

For a $J(3.91)=\frac{5}{2}$ assignment, the angular distribution calculated assuming pure quadrupole radiation for both members of the cascade is,[22]

$$W(\theta)=1+0.286P_2(\cos\theta)+0.381P_4(\cos\theta).$$

The presence of a large $P_4(\cos\theta)$ term is clearly inconsistent with the measured distribution. We note, however, that the coefficient A_4 can be zero if there is an $\sim$8% admixture of octupole intensity to a basically quadrupole component in either the upper or lower member of the cascade. The former is ruled out from the radiative width of the 4.85-MeV transition, which also restricts the parity to be even for a $J=\frac{5}{2}$ assignment. For an assumed $E2$-$M3$ mixture in the second member of the cascade (of an intensity to make $A_4=0$) the coefficient A_2 is then predicted to have a value $A_2\sim-0.2$, in contrast to the measured value $A_2=0.22\pm0.03$. On the basis of these considerations, we exclude the $J=\frac{5}{2}$ assignment from further considerations.

For an assumed $J=\frac{3}{2}$ assignment with a pure dipole primary transition the correlation function has the form[22]

$$W(\theta)=1+\frac{1-2\sqrt{3}\delta-\delta^2P_2(\cos\theta)}{4(1+\delta^2)},$$

where δ is the multipole amplitude ratio in the second member of the cascade. The experimental data may be fitted for values $\delta\sim0$ or $\delta\sim-2$. The former value is consistent with either positive or negative parity for the intermediate state, while the latter suggests a preference for an even parity assignment.

III. INVESTIGATION OF THE 1169-keV RESONANCE LEVEL

A. Branching-Ratio Determinations

The investigation of the decay scheme of the 1169-keV resonance level ($E_{ex}=9.07$ MeV) was aided considerably by the availability of a TMC 16 384-channel analyzer used in the study of the γ-γ coincidence spectra. In other respects the experimental procedure was similar to that described for the 849-keV resonance level.

Figure 12 shows the resonance gamma-ray spectra measured with a 5-in.$\times$5in. NaI(Tl) detector. A target gas pressure of 6 cm Hg was used for these measurements. The resonance was observed as a peak $\sim$50 keV in width with a ratio of peak-to-background (for $E_\gamma>2$

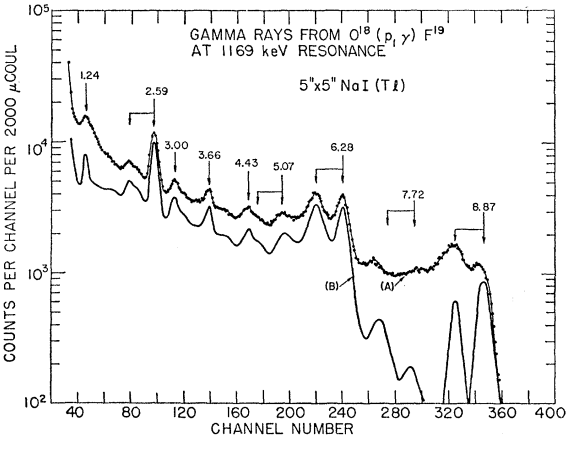

FIG. 12. Gamma-ray spectra measured at the 1169-keV resonance in $O^{18}+p$. Curve A shows the on-resonance spectrum, while curve B shows the resulting spectrum after subtraction of non-resonance components. Energies of prominent peaks are given in mega-electron-volts.

[22] W. T. Sharpe, J. M. Kennedy, B. J. Sears, and M. G. Hoyle, Chalk River Report CRT-556, 1964 (unpublished).

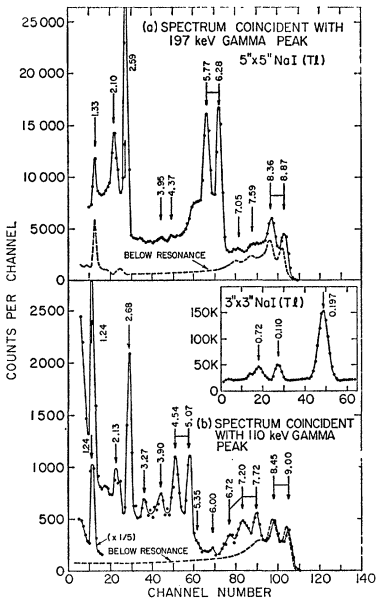

FIG. 13. Coincidence spectra measured at the 1169-keV resonance in $O^{18}+p$. Plots (a) and (b) show the higher-energy gamma spectra in coincidence with deexcitation gamma rays from the 197- and 110-keV levels of F^{19}. The low-energy spectrum is shown in the insert. Prominent peaks are labeled according to their energies (in mega-electron volts). The correspondence of full-energy and first-escape peaks for the higher energy transitions is indicated.

MeV) of about 4 to 1. Curve A of Fig. 12 shows the gamma-spectrum measured at the resonance peak. Curve B presents the spectrum obtained after subtracting the nonresonant contribution to A, and shows more clearly those transitions which can be assigned with certainty to the decay of the 1169-keV resonance level. The 1.24-, 2.59-, 5.07-, 6.28-, 7.72-, and 8.87-MeV gamma rays arise from deexcitation of the 9.07-MeV level through well-known levels of F^{19}, as will be demonstrated more clearly in the coincidence measurements reported in the following section. A series of measurements carried out for various proton energies between 1100 and 1250 keV, and also for different target thicknesses, demonstrates that the 3.00- and 3.66-MeV gamma rays exhibit the same resonance behavior as the 2.59- and 6.28-MeV gamma rays, while the 4.43-MeV gamma ray does not. The latter is due to the $N^{15}(p,\alpha\gamma)C^{12}$ reaction which has a well-known resonance[20] at 1210 keV with a width $\Gamma=23$ keV. The 3.66- and 3.00-MeV gamma rays have been seen also in previous measurements[10,15] which utilized both gas and solid targets under different experimental conditions, and thus additional evidence for their assignment to F^{19} is available. In the absence of coincidence measurements however their placement in the level scheme is uncertain.[15]

The results of the γ-γ coincidence measurements are shown in Fig. 13. These data were obtained using a TMC 16384-channel analyzer to record coincidence pulses from two NaI(Tl) detectors, one of which (a 5-in. $\times$5-in. detector) was set to view the high-energy spectrum corresponding to $E_\gamma \leqslant 10$ MeV, while the other (a 3-in. detector) was set to view the region $E_\gamma \leqslant 550$ keV. The resultant matrix of coincidence counts was subsequently summed over various rows and columns to permit examination of features of interest. Figure 13 shows the coincidence spectrum thus recorded by the 5-in.$\times$5-in. detector in coincidence (a) with the 197-keV gamma peak and (b) with the 110-keV gamma peak as viewed by the 3-in.$\times$3-in. detector. The insert shows the 110- and 197-keV peaks found in the spectrum recorded with the 3-in.$\times$3-in. detector. The various peaks evident in Fig. 13 are labeled according to an energy calibration based primarily on the positions of the 6.28- and 2.59-MeV peaks. On the basis of their energies and relative intensities the prominent lines have been fitted into the decay scheme shown in Fig. 14. Relative intensities and subsequently branching ratios were calculated primarily from the coincidence data of Fig. 13, using peak efficiencies for the 3-in.$\times$3-in. and 5-in.$\times$5-in. NaI(Tl) dectecors, and incorporating necessary absorption corrections for the 110- and 197-keV gamma rays. The previously established decay modes, spins, and parities of the five lowest lying states of F^{19} are also indicated. (The indicated restrictions on spins and parities for the higher lying levels are discussed in the following section.) The fact that the de-excitation of the levels at 1.35-, 1.46-, 1.56- and 2.79-MeV leads predominantly to one or the other of the levels at 110 and 197 keV was of considerable help in disentangling the coincidence spectra of Fig. 13. For example, the 2.79-MeV level is known to de-excite $\sim$100% to the 197-keV level. The relative intensities of the 6.28- and 2.59-MeV gamma rays in both the singles spectra of Fig. 12 and in the coincidence data of Fig. 13 are equal within their errors, and hence an average value of 64 ± 4 is quoted for the $9.07 \rightarrow 2.79$ branch. Similarly, the 7.72- and 1.24-MeV members of the $9.07 \rightarrow 1.35 \rightarrow 0.11$ cascade are also equal, and the branching ratio is calculated from the average relative intensity. Again, the 5.07- and 2.68-, and 2.90-MeV gamma rays are uniquely fitted into the level scheme as cascade transitions through the 4.00-MeV level; the energy resolution is adequate in

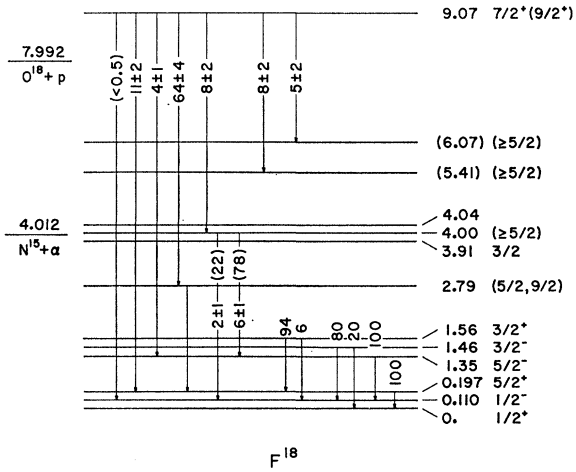

FIG. 14. Decay scheme for the 9.07-MeV level of F^{19}. The branching ratios and spin assignments for the first six levels are taken from the literature. The remainder summarize the results of the present measurements as discussed in the text.

TABLE I. Results of angular-distribution measurements for the 1169-keV resonance level in F^{19}.

E_γ (MeV)	Transition	A_2/A_0	A_4/A_0
6.28	9.07 → 2.79	−0.194±0.037	
2.59	2.79 → 0.20	+0.393±0.030	−0.167±0.043
3.7	9.07 →(5.4)	−0.60 ±0.11	
8.87	9.07 → 0.20	−0.06 ±0.14	
~9	(nonresonant)	−0.21 ±0.04	

this case to determine that it is the 4.00-MeV level and not the 4.04- or 3.91-MeV levels involved in this cascade. There is no evidence for a direct transition to the 110-keV level, while the data of Fig. 13(a) indicate that a significant fraction of the ~8.87-MeV gamma-rays feeding the 197-keV level are nonresonant. The coincidence data of Fig. 13 show clearly that the 3.0- and 3.7-MeV gamma rays (seen in the singles spectrum of Fig. 12) cannot arise as members of a triple cascade through the lower-lying levels of F^{19}, since all of the levels up to 4.0 MeV de-excite strongly through the 110- and 197-keV levels. Neither can they arise as members of a two-step cascade leading to the ground state, since the higher members of such a possible cascade are entirely absent in the singles spectrum of Fig. 12. Hence we are led to conclude that they arise as primary transitions from the 9.07-MeV level to higher lying states of F^{19} which in turn decay (most probably) by alpha-emission to N^{15}. The uncertainty in the determination of the energies of the 3.66- and 3.00-MeV gamma rays is about 15 keV, and hence an over-all uncertainty of ~25 keV is attached to the placement of the 5.41- and 6.07-MeV levels in the scheme shown in Fig. 14. With respect to previous work, the results summarized in the level scheme (Fig. 14) serve to confirm the assignments suggested previously for the origin of the 6.28-, 2.59-, 7.72-, and 8.87-MeV gamma rays. The presence of the 9.07 → 4.00 cascade elucidates the observations of Butler and Holmgren,[15] who found the intensity of the 1.24-MeV gamma ray to be appreciably stronger than that due to direct feeding of the 1.35-MeV level by the 7.72-MeV cascade transition.

The radiative width for the 9.07 → 2.79 transition determined in the present work is $\Gamma_\gamma(9.07 \rightarrow 2.79) = 0.84 \pm 0.19$ eV which gives a total radiative width for the level of $\Gamma_\gamma(9.07) = 1.31 \pm 0.31$ eV. These values are derived from the absolute yield of the 6.28- and 2.59-MeV gamma rays from the isotopically pure O^{18} target and incorporate the branching ratios given in Fig. 14. The values $(J+\frac{1}{2})\Gamma_p/\Gamma = 0.092$ and $\Gamma = 0.60 \pm 0.3$ keV are taken from the elastic scattering analysis of Yagi.[17]

We note here that the value quoted therein[17] $(J+\frac{1}{2}) \times \Gamma_p/\Gamma = 0.032 \pm 0.003$ is clearly inconsistent with the experimental elastic-scattering cross-section data,[14] and also with the (p,α) cross section $\sigma(\alpha_0) = 6 \pm 1.5$ mb measured by Amsel and Bishop.[18] For angles θ for which the incoherent term can be neglected, the general relationship between Γ_p/Γ and the maxima and minima of the elastic scattering cross section is given by[23]

$$(J+\tfrac{1}{2})P_i(\cos\theta) \times \Gamma_p/\Gamma = \lambda^{-1} \left| \sqrt{\sigma_{max}} - \sqrt{\sigma_{min}} \right| .$$

From the data of Fig. 9 in Ref. 14 we obtain the result $\Gamma_p/\Gamma \sim 0.02$, which also agrees with the (p,α_0) cross section. A more careful evaluation of this data gives $(J+\frac{1}{2})\Gamma_p/\Gamma = 0.09 \pm 0.01$ (where $J = \frac{7}{2}, \frac{9}{2}$) and it is this value we have used in determining $\Gamma_\gamma(9.07)$.

B. Angular-Distribution Measurements

The angular distributions of the prominent transitions evident in Fig. 12 were measured using a 5-in.×5-in. NaI(Tl) detector located at a distance of 16 cm from the target volume. The observed angular dependences of the peak intensities were then fitted with an (even order) Legendre polynomial expansion to determine the coefficients A_ν. The results, expressed as the ratios A_2/A_0 and A_4/A_0 are summarized in Table I. This procedure yields good results for the 6.28-, 2.59-, and 3.66-MeV gamma rays, but the 7.72-MeV transition is too weak to be studied in this way. The presence of the nonresonant 9-MeV radiation complicated the determination of the 8.87-MeV angular distribution. In this particular distribution measurement, a voltage gate was set to encompass the 8.87-MeV photo peak, and determinations of counting rates on-resonance and off-resonance were made for the various angles of observation. Since the 8.87-MeV transition is the only resonant gamma ray included in the voltage gate, this procedure then yields the angular distribution of the 8.87-MeV radiation, but to appreciably lesser accuracy than for the first-listed transitions. The angular distribution of the nonresonant contribution to the 9-MeV gate is also listed in Table I.

We note in passing that the relative yield of resonant/nonresonant radiation could be improved by using a thinner target, of the order of the resonance width $\Gamma < 1$ keV. In our measurements, however, the minimum target thickness (in keV) is restricted to be equal to or greater than the net straggling introduced by the proton energy loss in the entrance foil—in this case ~40–50 keV. This is roughly comparable to the target thickness used by Huang *et al.*[10] and hence their interpretation of the 7.72- and 8.87-MeV angular distributions is open to question, since apparently no account was taken of possible nonresonance contributions to the line intensities.

C. Results

In the following discussion we shall assume the $J = (\frac{7}{2},\frac{9}{2})^+$ assignment given to the 9.07-MeV state by Yagi.[17] The angular distribution of the 8.87-MeV gamma ray leading to the $J^\pi = \frac{5}{2}^+$ 0.197-MeV level then suggests a $J = \frac{7}{2}$ assignment for the 9.07-MeV resonance level as follows. If $J^\pi(9.07) = \frac{9}{2}^+$, then the transition

[23] R. A. Laubenstein and M. J. W. Laubenstein, Phys. Rev. 84, 18 (1951).

must proceed by an $E2$-$M3$ mixture. Significant admixtures of $M3$ are excluded by sum-rule considerations on the measured radiative width. Assuming pure $E2$ radiation, the angular distribution[22] is given by $W(\theta)=1+0.48P_2(\cos\theta)-0.29P_4(\cos\theta)$. In addition to predicting a large term in $P_4(\cos\theta)$ this distribution predicts a significant anisotropy of $\sim 50\%$ in the direction opposite to that observed in the present experiment. Conversely, for $J^\pi(9.07)=\frac{7}{2}^+$, the radiation is $M1$-$E2$ and the measured distribution can be fitted by reasonable mixtures of these two components.

Again, if $J^\pi(9.07)=\frac{9}{2}^+$, then the 7.72-MeV gamma ray proceeding to the 1.35-MeV, $J^\pi=\frac{5}{2}^-$ level must be $M2$ or $E3$ in character. If the radiation were pure $M2$, this would correspond to a strength $|M|^2=17$ Weisskopf units, which appears unreasonably large. Thus, the present experiment favors the assignment $J^\pi(9.07)=\frac{7}{2}^+$ on two counts. Indeed, were it not for the experimental uncertainty which attaches to the determination of the 8.87-MeV distribution coefficients, the results should exclude the $\frac{9}{2}^+$ possibility.

The primary motive in undertaking the distribution measurements, however, was to examine the restrictions which could be placed on possible spin-parity assignments for the 2.79-MeV level. As given previously,[10,11] various experimenters have shown that the 2.79-MeV level has $J\geqslant\frac{5}{2}$, and have suggested a $J=\frac{9}{2}$ assignment for this level. Definitive evidence has been obtained by Thomas, Lopes, Poletti, Ollerhead, and Warburton,[24] who (at Oxford) have studied 180° proton-gamma correlations in the $F^{19}(p,p'\gamma)F^{19}$ reaction and have thus eliminated all possible spin assignments save $J=\frac{5}{2}$ and $J=\frac{9}{2}$. The parity is, however, not determined by these experiments.

We investigate first the information contained in the angular distribution of the 2.59-MeV gamma ray. Since the most probable assignments for the two unknown levels involved in this cascade are $\frac{7}{2}^+(9.07)$ and $\frac{9}{2}(2.79)$ we consider these possibilities in detail as an example; considerations on the remaining possibilities are then presented in summary form. The angular-distribution coefficients for the 2.59-MeV gamma ray, assuming a $\frac{7}{2}\rightarrow\frac{9}{2}\rightarrow\frac{5}{2}$ spin sequence, are given as

$$\frac{A_2}{A_0}=\left(\frac{0.9167+0.6310\rho^2}{1+\rho^2}\right)\times\left(\frac{0.4762-1.2012\delta+0.4546\delta^2}{1+\delta^2}\right),$$

$$\frac{A_4}{A_0}=\left(\frac{0.7222-0.0281\rho^2}{1+\rho^2}\right)\times\left(\frac{-0.2857-1.8018\delta-0.0702\delta^2}{1+\delta^2}\right),$$

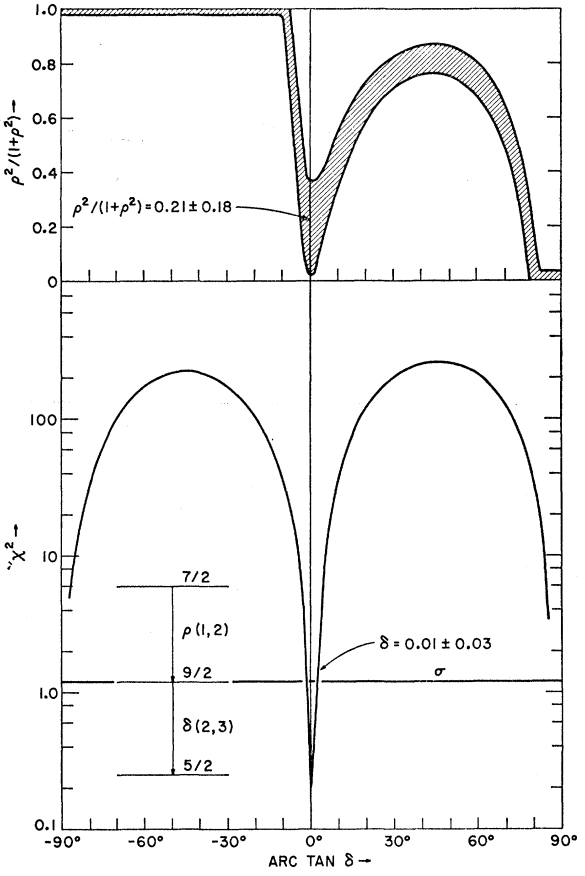

FIG. 15. Results of a χ^2 fit to the angular distribution data for the 2.59-MeV gamma ray arising from the $9.07\rightarrow 2.79\rightarrow 0.20$ transition following resonance formation of the 9.07-MeV level in $O^{18}+p$. The lower plot shows chi-squared as a function of δ, the mixing parameter in the $2.79\rightarrow 0.20$ transition, while the upper plot shows the corresponding solutions for the intensity mixing in the upper transition. The assumed spin sequence and notation are indicated in the insert. The 68% confidence limit corresponding to one standard deviation (σ) is indicated, as are the solutions for both δ and $\rho^2/(1+\rho^2)$.

where ρ is the multipole mixing parameter of the first (unobserved) transition $9.07\rightarrow 2.79$ ($L=1,2$) and δ is the multipole mixing parameter for the $2.79\rightarrow 0.197$ transition ($L=2,3$). The results of a chi-squared fit[25] to the experimentally determined coefficients A_2/A_0 and A_4/A_0 are shown in the lower half of Fig. 15. In this case the functions $1/(1+\rho^2)$ and $\rho^2/(1+\rho^2)$ which define the relative intensities of the two noninterfering multipoles involved in the first transition are treated as parameters. These parameters are then adjusted for a least-squares fit as δ is varied in steps across its range $-\infty\leqslant\delta\leqslant+\infty$. The resultant plot of χ^2 versus arctan δ shows minima at $\delta\sim 0$ and $|\delta|\cong\infty$. The latter solutions correspond to pure quadrupole radiation and can be excluded on the basis of the measurements of Thomas *et al.*[24] as indicated later. The upper plot of Fig. 15 shows the range of

[24] M. F. Thomas, J. S. Lopes, R. W. Ollerhead, A. R. Poletti, and E. K. Warburton, Nucl. Phys. (to be published).

[25] For presentation of fitting procedure, see A. R. Poletti and E. K. Warburton, Phys. Rev. 137, B595 (1965).

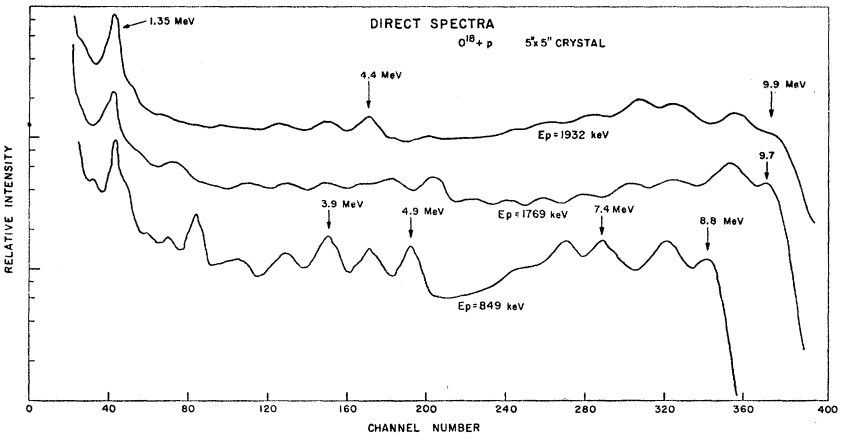

FIG. 16. $O^{18}+p$ direct gamma-radiation spectra obtained at the three proton energies $E_p=849$, 1769, and 1932 keV. Energies of prominent peaks are indicated in MeV.

$\rho^2/(1+\rho^2)$ allowed by the least-squares fit. The important feature evident here is that this quantity is not significantly different from zero, i.e., the data are not inconsistent with the upper transition being essentially dipole. These results are summarized in Table II, which includes also results of similar solutions for the remaining possible sequences. Shown in Table II for comparison are the solutions obtained by Thomas *et al.*[24] for the mixing parameter in the 2.79–0.197 transition. It is seen that there is good agreement between both solutions for δ, and hence we are not able to decide between the assignments $\frac{5}{2}$ or $\frac{9}{2}$ for the 2.79-MeV level.

All solutions are consistent with the assumption that the $9.07 \rightarrow 2.79$ de-excitation proceeds by the emission (predominantly) of the lowest order allowed multipole. This conclusion is also consistent with the results of the 6.28-MeV distribution data, which yields solutions $\rho=(-0.023\pm0.023)$ for $(\frac{7}{2}\rightarrow\frac{9}{2})$ and $\rho=(0.078\pm0.018)$ for $(\frac{7}{2}\rightarrow\frac{5}{2})$. We conclude therefore that simple distribution measurements do not uniquely determine either the spin or parity of the 2.79-MeV state. This is in contradiction to previous assertions.[10]

However, it is encouraging to note that the results of the present measurements are in excellent agreement with those of the Oxford group,[24] and serves to confirm their conclusions on possible multipole mixing amplitudes in the $2.79 \rightarrow 0.110$ transition. The present results also exclude a $J=\frac{7}{2}$ assignment, and a $J=11/2$ assignment appears unlikely in view of the strength of the higher order multipoles which must be assumed present to fit the angular distribution data.

Finally, from the radiative widths of the 5.07-, 3.66-, and 3.00-MeV transitions we conclude they must be predominantly dipole, and hence lead to levels having $J\geqslant\frac{5}{2}$. This is also consistent with the absence of a $P_4(\cos\theta)$ term in the 3.66-MeV angular distribution.

TABLE II. Mixing parameters for the $9.07 \rightarrow 2.79 \rightarrow 0.197$ transitions in F^{19} as determined from the angular distribution of the 2.59-MeV gamma ray.

Spin sequence (assumed)	Present experiment $\rho^2/(1+\rho^2)$	Present experiment δ	Oxford[a] δ
$\frac{7}{2}$-$\frac{9}{2}$-$\frac{5}{2}$	0.21±0.18	0.01±0.03	0.01±0.03
$\frac{9}{2}$-$\frac{9}{2}$-$\frac{5}{2}$	0.09±0.19	0.01±0.03	
$\frac{7}{2}$-$\frac{5}{2}$-$\frac{5}{2}$	0±0.05	−1.67±0.17	$-1.73^{+0.25}_{-0.23}$
$\frac{9}{2}$-$\frac{5}{2}$-$\frac{5}{2}$	0±0.05	−1.70±0.21	

[a] See Ref. 24.

IV. INVESTIGATION OF THE 1769- AND 1932-keV RESONANCES

The resonances at 1769 and 1932 keV in the $O^{18}(p,\gamma)$-F^{19} reaction have also received preliminary study. In agreement with earlier reports, it has been found that the 1769-keV resonance exhibits a very complex de-excitation. This is illustrated in Fig. 16. It is clear that many cascades involving levels in the 4- to 5-MeV range of excitation in F^{19} are involved, resulting in a rather featureless spectrum. The same is true of the de-excitation of the 1932-keV resonance for which a direct spectrum is also included in Fig. 16 along with the 849-keV direct spectrum for purposes of comparison. These spectra were measured under identical conditions with the entire system gain stabilizing on an 0.835-MeV line from a Mn^{54} source exposed to the spectrometer in parallel with the bombardment cell. Weak radiation at 4.43 MeV is evident in all spectra and is attributable to the prolific $N^{15}(p,\alpha)C^{12}$ reaction on the 0.37% abundant N^{15} component of a weak nitrogen contaminant of the O^{18} target gas.

No detailed attempt has been made, as yet, to establish more carefully the de-excitation of these two higher resonances; new instrumentation will be required to minimize these contaminants before reliable measurements on the weak cascades involving F^{19} states in this excitation range become possible.

V. DISCUSSION

A. Model Calculations for F^{19}

Extensive calculations utilizing a wide variety of models have already been alluded to in the Introduction.

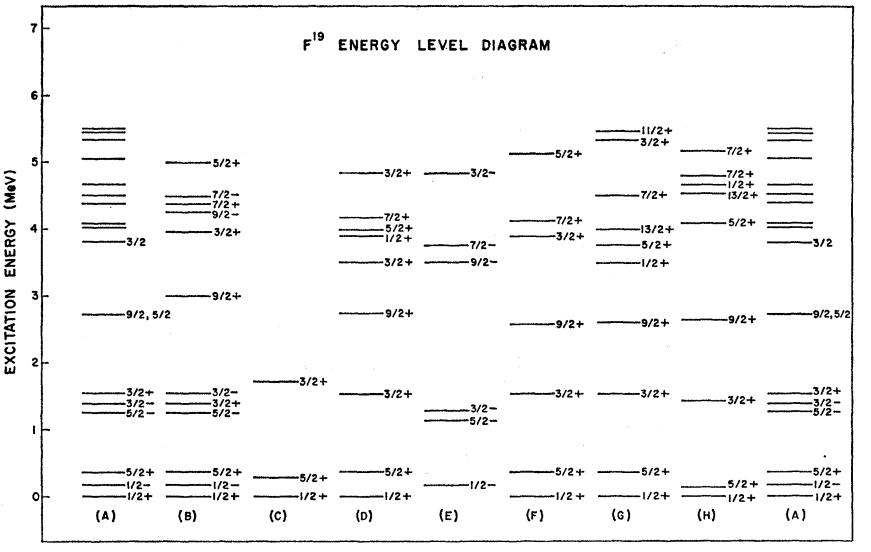

FIG. 17. Comparison of (A) the experimentally observed energy-level spectrum of F^{19} with the model-generated energy-level spectra of (B) Rakavy, (C) Redlich, (D) Chi and Davidson, (E) Harvey, (F) Paul, (G) Elliott and Flowers, and (H) Inoue *et al.*

The predicted level spectra of these calculations are presented in Fig. 17 for comparison with each other and with the experimental data now available. Of interest here are those calculations predicting a $\frac{3}{2}$ state in the energy region of 4 MeV, specifically the strong-coupling collective calculations and the SU_3 calculation.

A representative collective calculation is that of Paul[1] who achieved reasonable fits to the experimental data on the low-lying positive parity states of F^{19} by invoking strong Coriolis mixing of the $K^\pi=\frac{1}{2}^+$ and $\frac{3}{2}^+$ bands corresponding, within the framework of the Nilsson model, to intrinsic configurations with the odd proton occupying orbits 6 and 7, respectively. Paul found that the Coriolis mixing required to achieve agreement with the static level spectrum was extremely large. The $J=\frac{3}{2}$ member of the $K=\frac{1}{2}$ band, for example, was found to have 46% in intensity of $K=\frac{3}{2}$ configuration. Newton, Clegg, and Salmon,[26] on the other hand, conclude on the basis of their studies on inelastic scattering of 140-MeV protons on F^{19}, that the mixing must be much less than this, attributing Paul's overestimate of the mixing to the fact that the simple Nilsson model predicts too close a level spacing, hence too high a mixing, of the original pure K, $J=\frac{3}{2}$ configurations. These latter authors conclude that the $K=\frac{3}{2}$ and $\frac{1}{2}$ bands are only slightly mixed, but require that the parameter $\hbar^2/2I$ for both the positive and negative bands be $\sim$0.20 MeV rather than 0.30 MeV as assumed by Paul.

Harvey[8] has carried out a detailed SU_3 treatment of the low lying negative bands in F^{19} obtaining excellent accord with the experimentally observed $E3$ enhancement[27] ($|M|^2=12\pm4$) in the de-excitation of the $\frac{5}{2}^-$ state at 1.35 MeV is not reproduced. The remaining success of this treatment, which attributes the low-lying negative-parity states to promotion of a $p_{1/2}$ proton in the O^{16} core into the *sd* shell, lends credence to the corresponding rotational interpretation wherein a proton is promoted from Nilsson orbit 4 to fill orbit 6 thereby generating a $K^\pi=\frac{1}{2}^-$ band head. The alternative of generating such a configuration through promotion of the odd proton from orbit 6 to orbit 14 is not attractive because of the extreme deformation which would be required to bring down the energy of this configuration adequately.

B. Model Interpretations of the 3.91-MeV State

In considering the branching ratios shown in Fig. 10 it is of interest to utilize the simple Nilsson model, ignoring Coriolis mixing as suggested above, to obtain a qualitative understanding of the observed behavior. It is also of interest to consider the asymptotic form of the intrinsic wave functions involved and the states have been so labeled in Fig. 10 with the appropriate $|Nn_z\Lambda\rangle$ quantum numbers.[28] The positive and negative low excitation bands are characterized by $|220\rangle$ and $|101\rangle$, based on Nilsson orbits 6 and 4, respectively.

Within the spirit of this model the state at 3.91 MeV is then to be considered either as the positive parity band head corresponding to promotion of a proton from orbit 6 to orbit 7, with asymptotic quantum numbers $|211\rangle$, or as a negative parity band head with $K^\pi=\frac{3}{2}^-$ and $|101\rangle$ corresponding to the promotion of a proton from orbit 4 into orbit 6 and the coupling of the resultant $p_{1/2}$ hole to a $K=1$, rather than $K=0$, resultant of the two protons in the latter orbit. This type of $K=\frac{3}{2}^-$ hole configuration is also predicted by Harvey's SU_3 calculation at approximately 4.85 MeV, significantly above the excitation of the state under discussion.

[26] D. Newton, A. B. Clegg, and G. L. Salmon, Nucl. Phys. **55**, 353 (1964).

[27] A. E. Litherland, M. A. Clark, and C. Broude, Phys. Letters **3**, 204 (1963).

[28] B. R. Mottelson and S. G. Nilsson, Kgl. Danske, Videnskab. Selskab, Mat. Fys. Skriffer **1**, No. 8 (1959).

In terms of a simple Nilsson model the observed branching of the 3.91-MeV state is consistent with the positive parity assignment. The observed transitions, corresponding to $\Delta K=1$, $\Delta N=0$, $\Delta n_z=-1$, and $\Delta\Lambda=1$, do not violate the asymptotic selection rules for either $M1$ or $E1$ multipoles; moreover, $E1$ transitions to members of the negative parity band, whose apparent absence is *a priori* somewhat puzzling, would correspond to $\Delta K=1$, $\Delta N=1$, $\Delta n_z=1$, and $\Delta\Lambda=0$, violating the asymptotic selection rules $\Delta K=1$, $\Delta N=\pm 1$, $\Delta n_z=0$, and $\Delta\Lambda=1$ on two separate counts.

On the assumption of negative parity and a $|101\rangle$ configuration, it would be anticipated that relatively strong $M1$ transitions would be observed to the members of the $K^\pi=\frac{1}{2}^-$ band in addition to those to the members of the $\frac{1}{2}^+$ band, contrary to the experimental observation. Moreover, on this assumption of negative parity, the observed transitions into the $K^\pi=\frac{1}{2}^+$ rotational band would necessarily be $E1$ in character with $\Delta K=0$, $\Delta N=-1$, $\Delta n_z=-2$, and $\Delta\Lambda=1$ in violation of the Δn_z and $\Delta\Lambda$ asymptotic selection rules, so that $E1$ competition with the allowed $M1$ branches to the $K^\pi=\frac{1}{2}^-$ band would be further inhibited. Harvey[8] has noted that within the framework of his SU_3 model *all* $E1$ transition amplitudes vanish since the effective dipole operator may be written as $\mathbf{p}=Ze\mathbf{R}$, where $\mathbf{R}$ is the position vector for the center of mass of the proton distribution in the nucleus. To the extent that the center of mass of the proton distribution is in an S state, as it is for both negative and positive parity bands in the SU_3 model, $\mathbf{R}=0$ and the transition amplitudes vanish. Even if the restriction to a pure S state is relaxed, this assignment suggests marked inhibition of $E1$ transitions, as indeed is observed in the transition between the $K^\pi=\frac{1}{2}^-$ and $\frac{1}{2}^+$ band heads in F^{19}. Gale and Calvert[29] have shown, for example, that this transition is inhibited by a factor of 10^3 relative to single particle estimates. It should be noted that this latter transition also violates the asymptotic selection rules given by the Nilsson model.

The observed branching of the 3.91-MeV state is thus entirely consistent with a $\frac{3}{2}^+$ assignment to this state wherein the forbidden $E1$ transitions do not compete with allowed $M1$ (or $E2$) transitions. On the other hand, within the framework of this model the experimental data are in disagreement with a $\frac{3}{2}^-$ assignment since this would require that the forbidden $E1$ transitions completely mask any competition from allowed $M1$ transitions.

The absence of a third branch to the $\frac{5}{2}^+$ member of the $K=\frac{1}{2}^+$ band is somewhat puzzling. Considering only the dipole component of the transitions, and noting that (in the Nilsson notation) the terms involving the coefficients b_{M1} and b_{E2} vanish in this particular case, the $B(M1)$ ratios for the transitions into the ground-state band would be expected to be as follows:

$$(\tfrac{3}{2}\rightarrow\tfrac{1}{2}):(\tfrac{3}{2}\rightarrow\tfrac{3}{2}):(\tfrac{3}{2}\rightarrow\tfrac{5}{2})=1:0.8:0.2.$$

[29] N. H Gale and J. M. Calvert, Phys. Letters **1**, 348 (1963).

Experimentally, these ratios are found to be, after the appropriate E_γ^3 correction;

$$1:1.25:0.05.$$

The apparent enhancement of the $\frac{3}{2}\rightarrow\frac{3}{2}$ transition over the predictions of this simple model may well reflect the admixture of these two states, which as noted above is undoubtedly present if the 3.91-MeV state has positive parity. It should be noted in this connection that the $\frac{1}{2}^+$ ground state, on this basis, remains a pure configuration.

It is apparent from Fig. 17 that if the 3.91-MeV state has positive parity almost any variant of a collective model is able to predict the correct level ordering and to a rather surprising extent, at least up to and including the 3.91-MeV, $J=\frac{3}{2}$ state, the observed excitation energies. The shell model calculations of Elliott and Flowers,[3] of Redlich[4] and of Inoue *et al.*[7] on the other hand fail significantly with regard to prediction of the $\frac{3}{2}$ state at values of the central to spin-orbit strength ratio appropriate to the description of the lower positive parity excited states. Moreover, the dependence of the predicted excitation of a $\frac{3}{2}$ state on this ratio is anomalously slow in this energy region so that no reasonable modification of the ratio would suffice to bring this state down into agreement with the data presented herein.

C. Model Interpretations of the 8.76-MeV State

It follows necessarily, within any collective model, that the 849-keV resonance state studied here must be assigned $K^\pi=\frac{1}{2}^+$ since higher K bands exclude this J value. Although *a priori* at this excitation, it would be anticipated that state wave functions would be extremely complex, reflecting widespread configurational mixing, the case of the $J=\frac{1}{2}$ member of the $K^\pi=\frac{1}{2}^+$ band is somewhat anomalous in that mixing is only possible with another J^π, $K^\pi=\frac{1}{2}^+$, $\frac{1}{2}^+$ configuration. The anticipated low density of such configurations even at this excitation suggests that the configuration is relatively pure and certainly that the K quantum number remains pure.

It is of interest to consider the relevance of the model-dependent asymptotic quantum-number selection rules[28] to the de-excitation branching ratios of the 8.76-MeV resonance state itself. The experimental branching ratios displayed in Fig. 10 includes strong $E1$ transitions into the low lying $K^\pi=\frac{1}{2}^-$ band, apparently inhibited $M1$ transitions into the low lying $K^\pi=\frac{1}{2}^+$ band (clearly in the case of the ground state transition), and an apparently allowed transition (presumed $M1$) as the primary transition to the 3.91-MeV state.

Assuming the $|Nn_z\Lambda K\rangle$ assignments of $|220\,\frac{1}{2}\rangle$, $|101\,\frac{1}{2}\rangle$ and $|211\,\frac{3}{2}\rangle$ noted previously for the positive and negative $K=\frac{1}{2}$ band heads and the 3.91-MeV state, respectively, and considering the asymptotic selection rules appropriate to the transitions above, it follows that an assignment of $|211\,\frac{1}{2}\rangle$ to the 849-keV resonance

encompasses the observed branching and, further, that such an orbit (orbit 9) is available in the appropriate energy region. Within such a framework the weak ground-state transition, if present at all, reflects violation of the $\Delta K=\Delta N=\Delta n_z=\Delta\Lambda=0$, $M1$ selection rules; likewise, the 19% transition from the resonance to the 1.56-MeV state would be expected to show strong $E2$ enhancement. Unfortunately it is not possible to separate experimentally the radiations in the second state of the cascade involving this transition from that of the stronger cascade via the 1.46-MeV state, so that angular correlation measurements to establish the multipolarity of the 19% transition are precluded. It is also impossible to obtain limits on this multipolarity by measuring the mixed correlation for the two cascades simultaneously. All other transitions observed are completely allowed as $M1$ or $E2$ radiations.

VI. SUMMARY

Angular distribution studies of gamma radiations following the 1169-keV resonant proton capture reaction $O^{18}(p,\gamma)F^{19}$ are inadequate to distinguish between the possible spin assignments, $\frac{5}{2}$ or $\frac{9}{2}$, for the 2.79-MeV state of F^{19}. They are in agreement, however, with studies elsewhere which limit the spin to either of these two values. The studies also serve to determine the possible amplitude ratios for multipole mixing in the $2.79\rightarrow 0.110$ transition. A preference is indicated by these data for a $J^\pi=\frac{7}{2}^+$ assignment to the 9.07-MeV resonance level, but $J^\pi=\frac{9}{2}^+$ cannot be rigorously excluded.

Examination of the de-excitation of the 849-keV resonance in the $O^{18}(p,\gamma)F^{19}$ reaction has permitted identification of a $\frac{3}{2}$ level at 3.91 MeV in F^{19} and has established the de-excitation branching both of this state and of the resonance. The observed features of this branching may be correlated by invoking the electromagnetic selection rules appropriate to the strongly deformed, asymptotic Nilsson model. In this model the low-lying positive and negative bands are assigned asymptotic quantum numbers $|N,n_z,\Lambda\rangle$ of $|220\rangle$ and $|101\rangle$ respectively corresponding to Nilsson orbits 6 and 4 based on $d_{5/2}$ and $p_{1/2}$ particle and hole configurations, respectively. From model-dependent arguments the 3.91-MeV level is identified as the positive parity base of a $K=\frac{3}{2}$ band with a $|211\rangle$ assignment; it is further suggested that the 8.76-MeV state is again the base of a $K=\frac{1}{2}$ band corresponding to Nilsson orbit 9 with a $|211\rangle$ assignment.

ACKNOWLEDGMENTS

The Yale authors (J.P.A., A.J.H., and D.A.B.) are indebted to Dr. D. E. Alburger for extending to them the hospitality of the Brookhaven National Laboratory and for making available to them much of the detection equipment used herein. Our appreciation is also expressed to Dr. E. K. Warburton for the computer programs used in analyzing the angular-distribution data, and to the members of the Oxford group for permission to quote their results prior to complete publication. We are also indebted to Robert Lindgren for his assistance in these measurements.